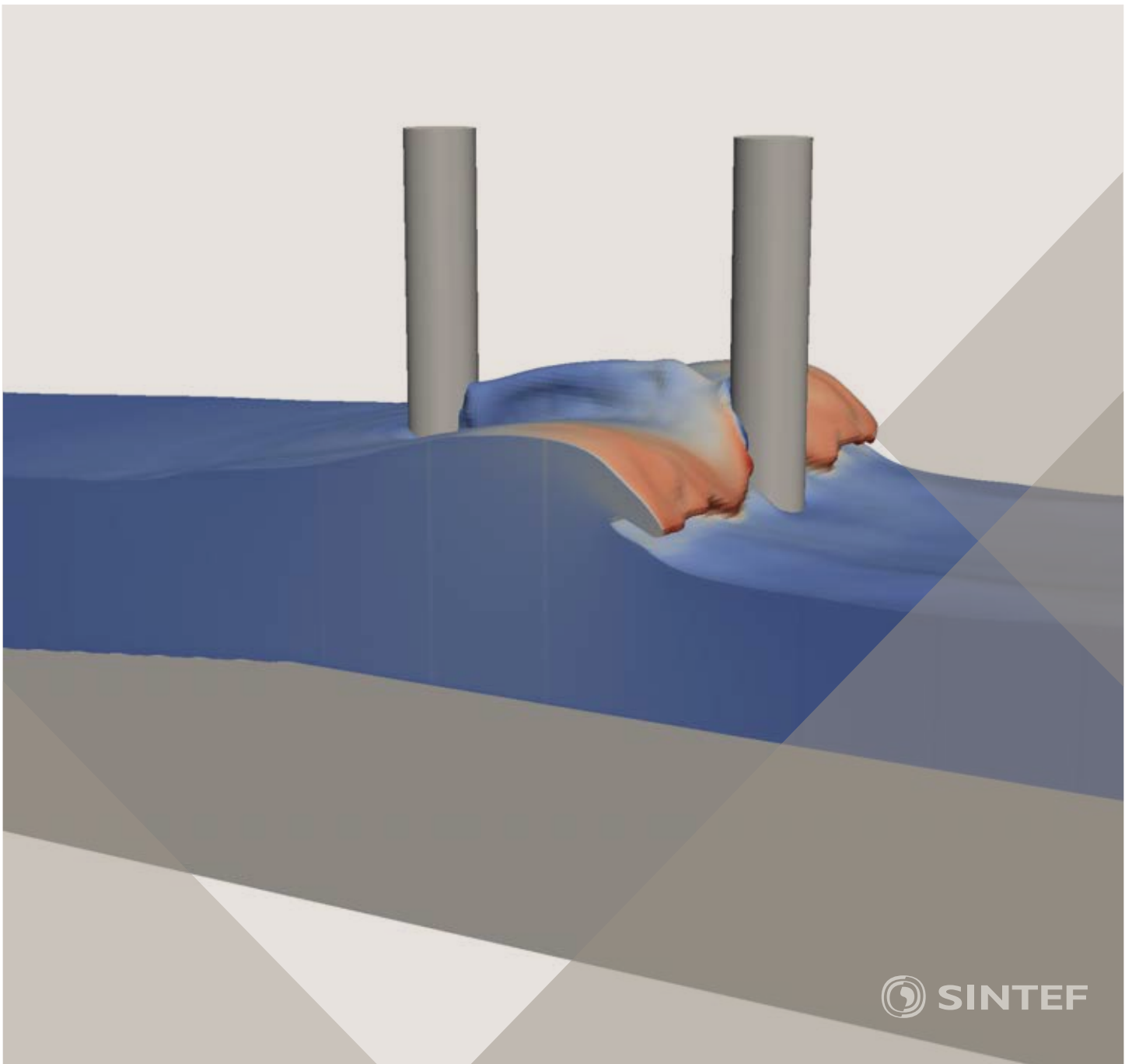


Proceedings of the 12<sup>th</sup> International Conference on  
Computational Fluid Dynamics in the Oil & Gas,  
Metallurgical and Process Industries

# Progress in Applied CFD – CFD2017



SINTEF Proceedings

Editors:

Jan Erik Olsen and Stein Tore Johansen

## **Progress in Applied CFD – CFD2017**

Proceedings of the 12<sup>th</sup> International Conference on Computational Fluid Dynamics  
in the Oil & Gas, Metallurgical and Process Industries

SINTEF Academic Press

SINTEF Proceedings no 2

Editors: Jan Erik Olsen and Stein Tore Johansen

**Progress in Applied CFD – CFD2017**

Selected papers from 10<sup>th</sup> International Conference on Computational Fluid Dynamics in the Oil & Gas, Metallurgical and Process Industries

Key words:

CFD, Flow, Modelling

Cover, illustration: Arun Kamath

ISSN 2387-4295 (online)

ISBN 978-82-536-1544-8 (pdf)

© Copyright SINTEF Academic Press 2017

The material in this publication is covered by the provisions of the Norwegian Copyright Act. Without any special agreement with SINTEF Academic Press, any copying and making available of the material is only allowed to the extent that this is permitted by law or allowed through an agreement with Kopinor, the Reproduction Rights Organisation for Norway. Any use contrary to legislation or an agreement may lead to a liability for damages and confiscation, and may be punished by fines or imprisonment

SINTEF Academic Press

Address:       Forskningsveien 3 B  
                  PO Box 124 Blindern  
                  N-0314 OSLO

Tel:             +47 73 59 30 00

Fax:            +47 22 96 55 08

[www.sintef.no/byggforsk](http://www.sintef.no/byggforsk)

[www.sintefbok.no](http://www.sintefbok.no)

**SINTEF Proceedings**

SINTEF Proceedings is a serial publication for peer-reviewed conference proceedings on a variety of scientific topics.

The processes of peer-reviewing of papers published in SINTEF Proceedings are administered by the conference organizers and proceedings editors. Detailed procedures will vary according to custom and practice in each scientific community.

## PREFACE

This book contains all manuscripts approved by the reviewers and the organizing committee of the 12th International Conference on Computational Fluid Dynamics in the Oil & Gas, Metallurgical and Process Industries. The conference was hosted by SINTEF in Trondheim in May/June 2017 and is also known as CFD2017 for short. The conference series was initiated by CSIRO and Phil Schwarz in 1997. So far the conference has been alternating between CSIRO in Melbourne and SINTEF in Trondheim. The conferences focuses on the application of CFD in the oil and gas industries, metal production, mineral processing, power generation, chemicals and other process industries. In addition pragmatic modelling concepts and bio-mechanical applications have become an important part of the conference. The papers in this book demonstrate the current progress in applied CFD.

The conference papers undergo a review process involving two experts. Only papers accepted by the reviewers are included in the proceedings. 108 contributions were presented at the conference together with six keynote presentations. A majority of these contributions are presented by their manuscript in this collection (a few were granted to present without an accompanying manuscript).

The organizing committee would like to thank everyone who has helped with review of manuscripts, all those who helped to promote the conference and all authors who have submitted scientific contributions. We are also grateful for the support from the conference sponsors: ANSYS, SFI Metal Production and NanoSim.

Stein Tore Johansen & Jan Erik Olsen



Organizing committee:

Conference chairman: Prof. Stein Tore Johansen

Conference coordinator: Dr. Jan Erik Olsen

Dr. Bernhard Müller

Dr. Sigrid Karstad Dahl

Dr. Shahriar Amini

Dr. Ernst Meese

Dr. Josip Zoric

Dr. Jannike Solsvik

Dr. Peter Witt

Scientific committee:

Stein Tore Johansen, SINTEF/NTNU

Bernhard Müller, NTNU

Phil Schwarz, CSIRO

Akio Tomiyama, Kobe University

Hans Kuipers, Eindhoven University of Technology

Jinghai Li, Chinese Academy of Science

Markus Braun, Ansys

Simon Lo, CD-adapco

Patrick Segers, Universiteit Gent

Jiyuan Tu, RMIT

Jos Derksen, University of Aberdeen

Dmitry Eskin, Schlumberger-Doll Research

Pär Jönsson, KTH

Stefan Pirker, Johannes Kepler University

Josip Zoric, SINTEF

## CONTENTS

<b>PRAGMATIC MODELLING .....</b>	<b>9</b>
On pragmatism in industrial modeling. Part III: Application to operational drilling .....	11
CFD modeling of dynamic emulsion stability .....	23
Modelling of interaction between turbines and terrain wakes using pragmatic approach .....	29
<b>FLUIDIZED BED .....</b>	<b>37</b>
Simulation of chemical looping combustion process in a double looping fluidized bed reactor with cu-based oxygen carriers.....	39
Extremely fast simulations of heat transfer in fluidized beds.....	47
Mass transfer phenomena in fluidized beds with horizontally immersed membranes .....	53
A Two-Fluid model study of hydrogen production via water gas shift in fluidized bed membrane reactors .....	63
Effect of lift force on dense gas-fluidized beds of non-spherical particles .....	71
Experimental and numerical investigation of a bubbling dense gas-solid fluidized bed .....	81
Direct numerical simulation of the effective drag in gas-liquid-solid systems .....	89
A Lagrangian-Eulerian hybrid model for the simulation of direct reduction of iron ore in fluidized beds.....	97
High temperature fluidization - influence of inter-particle forces on fluidization behavior .....	107
Verification of filtered two fluid models for reactive gas-solid flows .....	115
<b>BIOMECHANICS.....</b>	<b>123</b>
A computational framework involving CFD and data mining tools for analyzing disease in carotid artery .....	125
Investigating the numerical parameter space for a stenosed patient-specific internal carotid artery model.....	133
Velocity profiles in a 2D model of the left ventricular outflow tract, pathological case study using PIV and CFD modeling.....	139
Oscillatory flow and mass transport in a coronary artery.....	147
Patient specific numerical simulation of flow in the human upper airways for assessing the effect of nasal surgery.....	153
CFD simulations of turbulent flow in the human upper airways .....	163
<b>OIL &amp; GAS APPLICATIONS .....</b>	<b>169</b>
Estimation of flow rates and parameters in two-phase stratified and slug flow by an ensemble Kalman filter .....	171
Direct numerical simulation of proppant transport in a narrow channel for hydraulic fracturing application .....	179
Multiphase direct numerical simulations (DNS) of oil-water flows through homogeneous porous rocks .....	185
CFD erosion modelling of blind tees .....	191
Shape factors inclusion in a one-dimensional, transient two-fluid model for stratified and slug flow simulations in pipes .....	201
Gas-liquid two-phase flow behavior in terrain-inclined pipelines for wet natural gas transportation .....	207

<b>NUMERICS, METHODS &amp; CODE DEVELOPMENT .....</b>	<b>213</b>
Innovative computing for industrially-relevant multiphase flows .....	215
Development of GPU parallel multiphase flow solver for turbulent slurry flows in cyclone.....	223
Immersed boundary method for the compressible Navier–Stokes equations using high order summation-by-parts difference operators .....	233
Direct numerical simulation of coupled heat and mass transfer in fluid-solid systems .....	243
A simulation concept for generic simulation of multi-material flow, using staggered Cartesian grids.....	253
A cartesian cut-cell method, based on formal volume averaging of mass, momentum equations.....	265
SOFT: a framework for semantic interoperability of scientific software .....	273
 <b>POPULATION BALANCE .....</b>	 <b>279</b>
Combined multifluid-population balance method for polydisperse multiphase flows .....	281
A multifluid-PBE model for a slurry bubble column with bubble size dependent velocity, weight fractions and temperature.....	285
CFD simulation of the droplet size distribution of liquid-liquid emulsions in stirred tank reactors .....	295
Towards a CFD model for boiling flows: validation of QMOM predictions with TOPFLOW experiments .....	301
Numerical simulations of turbulent liquid-liquid dispersions with quadrature-based moment methods.....	309
Simulation of dispersion of immiscible fluids in a turbulent couette flow .....	317
Simulation of gas-liquid flows in separators - a Lagrangian approach.....	325
CFD modelling to predict mass transfer in pulsed sieve plate extraction columns .....	335
 <b>BREAKUP &amp; COALESCENCE .....</b>	 <b>343</b>
Experimental and numerical study on single droplet breakage in turbulent flow .....	345
Improved collision modelling for liquid metal droplets in a copper slag cleaning process .....	355
Modelling of bubble dynamics in slag during its hot stage engineering.....	365
Controlled coalescence with local front reconstruction method .....	373
 <b>BUBBLY FLOWS .....</b>	 <b>381</b>
Modelling of fluid dynamics, mass transfer and chemical reaction in bubbly flows .....	383
Stochastic DSMC model for large scale dense bubbly flows.....	391
On the surfacing mechanism of bubble plumes from subsea gas release.....	399
Bubble generated turbulence in two fluid simulation of bubbly flow .....	405
 <b>HEAT TRANSFER .....</b>	 <b>413</b>
CFD-simulation of boiling in a heated pipe including flow pattern transitions using a multi-field concept .....	415
The pear-shaped fate of an ice melting front .....	423
Flow dynamics studies for flexible operation of continuous casters (flow flex cc).....	431
An Euler-Euler model for gas-liquid flows in a coil wound heat exchanger.....	441
 <b>NON-NEWTONIAN FLOWS.....</b>	 <b>449</b>
Viscoelastic flow simulations in disordered porous media .....	451
Tire rubber extrudate swell simulation and verification with experiments .....	459
Front-tracking simulations of bubbles rising in non-Newtonian fluids.....	469
A 2D sediment bed morphodynamics model for turbulent, non-Newtonian, particle-loaded flows.....	479

<b>METALLURGICAL APPLICATIONS.....</b>	<b>491</b>
Experimental modelling of metallurgical processes .....	493
State of the art: macroscopic modelling approaches for the description of multiphysics phenomena within the electroslag remelting process .....	499
LES-VOF simulation of turbulent interfacial flow in the continuous casting mold .....	507
CFD-DEM modelling of blast furnace tapping .....	515
Multiphase flow modelling of furnace tapholes .....	521
Numerical predictions of the shape and size of the raceway zone in a blast furnace.....	531
Modelling and measurements in the aluminium industry - Where are the obstacles? .....	541
Modelling of chemical reactions in metallurgical processes.....	549
Using CFD analysis to optimise top submerged lance furnace geometries .....	555
Numerical analysis of the temperature distribution in a martensitic stainless steel strip during hardening.....	565
Validation of a rapid slag viscosity measurement by CFD.....	575
Solidification modeling with user defined function in ANSYS Fluent.....	583
Cleaning of polycyclic aromatic hydrocarbons (PAH) obtained from ferroalloys plant.....	587
Granular flow described by fictitious fluids: a suitable methodology for process simulations .....	593
A multiscale numerical approach of the dripping slag in the coke bed zone of a pilot scale Si-Mn furnace.....	599
<b>INDUSTRIAL APPLICATIONS .....</b>	<b>605</b>
Use of CFD as a design tool for a phosphoric acid plant cooling pond .....	607
Numerical evaluation of co-firing solid recovered fuel with petroleum coke in a cement rotary kiln: Influence of fuel moisture .....	613
Experimental and CFD investigation of fractal distributor on a novel plate and frame ion-exchanger .....	621
<b>COMBUSTION .....</b>	<b>631</b>
CFD modeling of a commercial-size circle-draft biomass gasifier.....	633
Numerical study of coal particle gasification up to Reynolds numbers of 1000.....	641
Modelling combustion of pulverized coal and alternative carbon materials in the blast furnace raceway .....	647
Combustion chamber scaling for energy recovery from furnace process gas: waste to value .....	657
<b>PACKED BED.....</b>	<b>665</b>
Comparison of particle-resolved direct numerical simulation and 1D modelling of catalytic reactions in a packed bed .....	667
Numerical investigation of particle types influence on packed bed adsorber behaviour .....	675
CFD based study of dense medium drum separation processes .....	683
A multi-domain 1D particle-reactor model for packed bed reactor applications.....	689
<b>SPECIES TRANSPORT &amp; INTERFACES .....</b>	<b>699</b>
Modelling and numerical simulation of surface active species transport - reaction in welding processes .....	701
Multiscale approach to fully resolved boundary layers using adaptive grids.....	709
Implementation, demonstration and validation of a user-defined wall function for direct precipitation fouling in Ansys Fluent.....	717

<b>FREE SURFACE FLOW &amp; WAVES .....</b>	<b>727</b>
Unresolved CFD-DEM in environmental engineering: submarine slope stability and other applications.....	729
Influence of the upstream cylinder and wave breaking point on the breaking wave forces on the downstream cylinder .....	735
Recent developments for the computation of the necessary submergence of pump intakes with free surfaces .....	743
Parallel multiphase flow software for solving the Navier-Stokes equations .....	752
 <b>PARTICLE METHODS .....</b>	 <b>759</b>
A numerical approach to model aggregate restructuring in shear flow using DEM in Lattice-Boltzmann simulations .....	761
Adaptive coarse-graining for large-scale DEM simulations.....	773
Novel efficient hybrid-DEM collision integration scheme.....	779
Implementing the kinetic theory of granular flows into the Lagrangian dense discrete phase model.....	785
Importance of the different fluid forces on particle dispersion in fluid phase resonance mixers .....	791
Large scale modelling of bubble formation and growth in a supersaturated liquid.....	798
 <b>FUNDAMENTAL FLUID DYNAMICS .....</b>	 <b>807</b>
Flow past a yawed cylinder of finite length using a fictitious domain method .....	809
A numerical evaluation of the effect of the electro-magnetic force on bubble flow in aluminium smelting process.....	819
A DNS study of droplet spreading and penetration on a porous medium.....	825
From linear to nonlinear: Transient growth in confined magnetohydrodynamic flows.....	831

## DIRECT NUMERICAL SIMULATION OF PROPPANT TRANSPORT IN A NARROW CHANNEL FOR HYDRAULIC FRACTURING APPLICATION

R. V. MAITRI<sup>1\*</sup>, I. KOIMTZOGLU<sup>1</sup>, S. DAS<sup>1</sup>, J.A.M. KUIPERS<sup>1</sup>, J.T. PADDING<sup>2</sup>, E.A.J.F. PETERS<sup>1</sup>

<sup>1</sup>Multiphase Reactors Group, Department of Chemical Engineering and Chemistry,  
 Eindhoven University of Technology, THE NETHERLANDS

<sup>2</sup>Intensified Reaction & Separation Systems, Process and Energy Department,  
 Delft University of Technology, THE NETHERLANDS

\* E-mail: r.maitri@tue.nl

### ABSTRACT

An efficient and accurate model for the direct numerical simulations (DNS) of liquid-solid flows is presented in this work. In this numerical model, fluid-solid coupling is achieved by implementing the no-slip boundary condition at the particles' surfaces by using a second order ghost-cell immersed boundary method, allowing for a fixed Cartesian grid to be used for solving the fluid equations. The particle-particle and particle-wall interactions are implemented using the soft sphere collision model. Lubrication forces are included through a sub-grid scale model because of its range of influence on a scale smaller than the grid size.

After the validation of the model, the transport of solid particles in a narrow channel is simulated to mimic the proppant transport in rock fractures in fracking process. The simulations are performed for solids volume fractions ranging from 1.7 to 20 % with the range of Reynolds and Archimedes number: 100-400 and 0-7848, respectively.

**Keywords:** Direct Numerical Simulation (DNS), Immersed Boundary Method (IBM), Multiphase flow, fracking

### NOMENCLATURE

#### Greek Symbols

$\varepsilon_s$	Solids volume fraction
$\mu$	Dynamic viscosity, [kg/m.s]
$\xi_s$	Dimensionless distance
$\rho$	Density, [kg/m <sup>3</sup> ]
$\tau$	Viscous stress, [N/m <sup>2</sup> ]
$\phi$	Variable in the equation to be solved
$\bar{\omega}, \bar{\Omega}$	Rotational velocity, [1/s]

#### Latin Symbols

$a$	Coefficients in discretized equation
$Ar$	Archimedes number
$b_c$	Explicit part in the discretized equation
$D$	Diameter, [m]
$\bar{F}_{f \rightarrow s}$	Force exerted by fluid on solid, [N]
$\bar{F}_{s \rightarrow s}$	Force in solid-solid interaction, [N]
$\bar{g}$	Gravitational acceleration, [m/s <sup>2</sup> ]
$H$	Height of the channel, [m]
$I$	Moment of inertia, [kg.m <sup>2</sup> ]
$m$	Mass, [kg]
$\bar{n}$	Unit normal vector,
$N$	Total number of particles

$p$	Pressure, [N/m <sup>2</sup> ]
$\bar{r}$	Position vector, [m]
$Re$	Reynolds number
$St$	Stokes number
$t$	Time, [s]
$\bar{T}_{f \rightarrow s}$	Torque exerted by fluid on solid, [N.m]
$\bar{u}$	Fluid velocity, [m/s]
$\bar{w}$	Translational velocity, [m/s]
$\bar{y}$	Vertical height [m]

#### Sub/superscripts

$f$	Fluid phase
$p$	Particle
$s$	Solid phase

#### Operators

$\nabla$	Gradient [1/m]
$\nabla \cdot$	Divergence [1/m]
$\nabla^2$	Laplace [1/m <sup>2</sup> ]

### INTRODUCTION

Particle laden flows are encountered in many industrial as well as natural processes. These include proppant transport in fracking, biological flows, sediment transport in river and environmental flows. The fundamental understanding of fluid-solid multiphase flows is important for the optimization of these processes and computational fluid dynamics (CFD) is an effective numerical tool to obtain an insight in such complex processes.

For fluid-solid interaction, the immersed boundary method (Peskin, 1972) was introduced to couple the movement of the flexible membrane and the fluid around it. This method used the feedback forcing method to enforce the no-slip boundary condition on the particle surface. A different approach was proposed by (Fadlun *et al.*, 2000) to have a direct forcing to impose the no-slip boundary condition. (Uhlmann, 2005) combined the direct forcing method with the regularized delta function to remove oscillations in moving particles' simulation. This method was improved later (Breugem, 2012; Kempe and Fröhlich, 2012) to account for the lower solid to fluid density ratios and to improve the order of accuracy of the original method. Another efficient variant of the IBM named ghost cell method (Tseng and Ferziger, 2003) is also often used. Here the ghost node inside the solid is given a velocity to impose the no-slip boundary condition

on the particle surface. This method was later modified and extended for moving particles in fluidized beds (Deen *et al.*, 2012) and is used with further modification in this paper for the simulations.

Particle laden flows can be categorized in two classes: free-surface flow like sediment transport in a river and narrow channel flow like proppant transport in a rock fracture. The relevant length scales and the flow structures in both the phenomena are quite different to each other. This work focuses on the narrow channel flow to obtain an insight into the proppant transport phenomenon. Previous numerical studies of particle transport in a narrow channel were performed for 2D circular particles using Arbitrary-Lagrangian-Eulerian (ALE) method (Choi and Joseph, 2001; Patankar *et al.*, 2001). In this paper, fully resolved 3D simulations are performed to capture the effect of flow structures in the transverse direction as well.

## MODEL DESCRIPTION

Our DNS model solves the coupled fluid-solid flow where the fluid phase is governed by continuity and Navier-Stokes equation and the solid motion is governed by Newton-Euler equations. The mathematical formulation of these equations is as follows (Eq. 1 - 4):

### Fluid phase:

The governing equations for incompressible Newtonian fluid flow are:

$$(\nabla \cdot \bar{u}) = 0 \quad (1)$$

$$\frac{\partial \rho_f \bar{u}}{\partial t} + (\nabla \cdot \rho_f \bar{u} \bar{u}) = -\nabla p + \mu_f \nabla^2 \bar{u} + \rho_f \bar{g} \quad (2)$$

The viscous term in the Navier-Stokes equation is discretized with the standard second-order central difference scheme. For the convective terms, the total variation diminishing minmod scheme is used, with a deferred correction. In the deferred correction, first order upwind (FOU) is implemented implicitly and the corrector step is carried out explicitly. The velocity and pressure variable are solved on a staggered grid with the standard fractional step method.

### Solid phase:

The translational and rotational motion of particles is governed by the following equations:

$$m_p \frac{d\bar{w}_p}{dt} = m_p \bar{g} + \bar{F}_{f \rightarrow s} + \bar{F}_{s \rightarrow s} \quad (3)$$

$$I_p \frac{d\bar{\omega}_p}{dt} = \bar{T}_{f \rightarrow s} \quad (4)$$

The force and torque exerted by the fluid on a spherical particle is:

$$\bar{F}_{f \rightarrow s} = - \iint_{S_p} (\tau_f \cdot \bar{n} + p \bar{n}) dS \quad (5)$$

$$\bar{T}_{f \rightarrow s} = - \iint_{S_p} (\bar{r} - \bar{r}_p) \times (\tau_f \cdot \bar{n}) dS \quad (6)$$

The particle-particle interaction ( $\bar{F}_{s \rightarrow s}$ ) is accounted for by the standard soft-sphere collision (Cundall and Strack, 1979) for the normal forces whereas a sub-grid scale lubrication model (Brenner, 1961) is used for the correction of the unresolved hydrodynamic interaction between particles.

## Fluid-solid interaction

The fluid-solid interaction takes place through momentum exchange at the particle surface and is incorporated in this study using the second order ghost-cell immersed boundary method (Deen *et al.*, 2012; Das *et al.*, 2016). In this method, the no-slip boundary condition on the particle surface is enforced implicitly by modifying the coefficient matrix of the fluid velocities at the level of the discrete equivalent of Eq. 2. In Fig. 1,  $\phi_i$  denotes a flow variable in cell at position  $i$ , such as a velocity component. The velocity at ghost cell 0 in Fig. 1 is extrapolated based on the particle velocity and the neighbouring fluid velocities and is represented as:

$$\phi_0 = -\frac{2\xi_s}{1-\xi_s} \phi_1 + \frac{\xi_s}{2-\xi_s} \phi_2 + \frac{2}{(1-\xi_s)(2-\xi_s)} \phi_p \quad (7)$$

It can be noted that the velocity at point  $\phi_1$  and  $\phi_2$  are to be solved for the new time step as well and hence, the extrapolation modifies the coefficients for the equation of velocity at  $\phi_1$ . The generic form of the discretized momentum equation and the updated coefficients are given in Eq. 8 - 11, where  $a_i$  and  $b_i$  indicate the coefficients and the explicit terms, respectively, before incorporating boundary conditions at the fluid-solid interface and  $\hat{a}_i$  and  $\hat{b}_i$  are the modified values after IBM implementation.

$$a_1 \phi_1 + \sum_{nb} a_{nb} \phi_{nb} = b_c \quad (8)$$

$$\hat{a}_1 = a_1 - a_0 \frac{2\xi_s}{1-\xi_s} \quad (9)$$

$$\hat{a}_2 = a_2 + a_0 \frac{\xi_s}{2-\xi_s} \quad (10)$$

$$\hat{b}_c = b_c - a_0 \frac{2}{(1-\xi_s)(2-\xi_s)} \phi_p \quad (11)$$

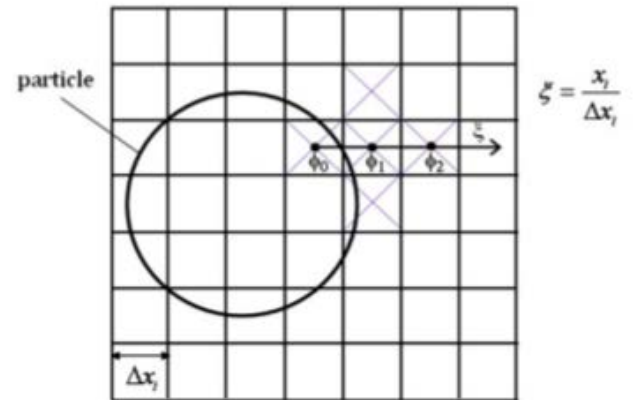


**Figure 1:** Representation of the fluid-solid interface on the Cartesian grid (Deen *et al.*, 2012)

## VERIFICATION AND VALIDATION

The original IBM (Deen *et al.*, 2012) is modified to compute the torque on spherical particles accurately. The performance of the new algorithm is quantified by comparing the torque computations with the analytical solution of the slowly rotating sphere in a large body of quiescent fluid in a creeping flow regime (Fig. 2) and the sedimentation of a single particle in a box filled with the liquid.

## Torque on a sphere

The torque on a sphere in a creeping flow (Bird *et al.*, 2007):

$$T = \pi\mu_f\omega_p D_p^3 \quad (12)$$

The results of the improved IBM method are presented in the Table 1. It is found that the error associated with the torque computation is reduced by 3-13 times (depending on the resolution) after the implementation of an improved algorithm. The accurate torque computation is very important in the particle laden flows as the particle rotation affects the fluid flow which in turn affects the particles again and hence, the small error can amplify over the time.

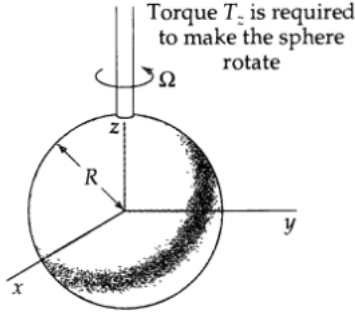


**Figure 2:** Freely rotating sphere in the quiescent fluid (Bird *et al.*, 2007)

**Table 1:** Error estimation of the numerical values of torque with the original and improved IBM ( $\mu_f = 2 \text{ kg/m.s}$ ,  $\omega = 10^{-5} \text{ s}^{-1}$ ,  $D_p = 0.2 \text{ m}$ ),  $\text{Torque}_{analytical} = 5.03 \times 10^{-7} \text{ N.m}$

$D_p/\Delta x$	Torque (N.m)		% Error	
	Original	Improved	Original	Improved
10	$4.52 \times 10^{-7}$	$4.86 \times 10^{-7}$	10.14 %	3.31 %
20	$4.60 \times 10^{-7}$	$4.96 \times 10^{-7}$	8.55 %	1.29 %
40	$4.88 \times 10^{-7}$	$5.00 \times 10^{-7}$	2.98 %	0.47 %
80	$4.92 \times 10^{-7}$	$5.02 \times 10^{-7}$	2.2 %	0.17 %

## Sedimentation of a single particle

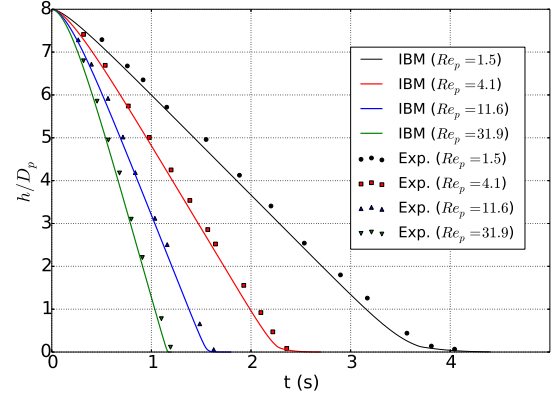
As a next validation case, numerical simulation of a single particle sedimentation in a large box is performed and the results are compared with the experimental measurements (Ten Cate *et al.*, 2002). The simulation is carried out in the domain of the size  $6.67D_p \times 10.67D_p \times 6.67D_p$  with initial particle centre position at  $8.5D_p$  from the bottom wall. The diameter of the particle is 0.015 m and the density is 1120  $\text{kg/m}^3$ . Free-slip boundary condition is applied on the walls for velocity. The comparison results for the position of the bottom surface of the particle from bottom wall and its vertical velocity are presented in Fig. 3. An excellent agreement between the simulation and experimental results is obtained.

## RESULTS

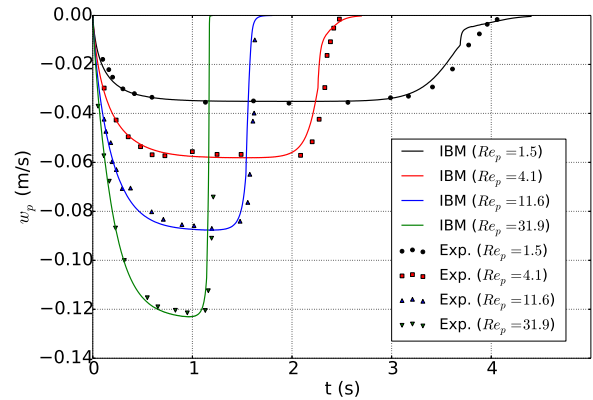
To mimic the proppant transport phenomenon in rock fractures, multi-particle simulations in the narrow channel are performed in this paper. Especially, the influence of the initial particle configuration and the solids volume fraction is studied. The transport of particles is governed by the two important non-dimensional numbers:

**Table 2:** The details of the simulation for single particle sedimentation case

Case	$Re_p$	St	$\rho_f$	$\mu_f$
1	1.4	0.19	970	0.373
2	4.1	0.53	965	0.212
3	11.6	1.50	962	0.113
4	31.9	4.13	960	0.058



a) Particle location



b) Particle velocity

**Figure 3:** Comparison of numerical simulation with the experimental results for the case of single particle sedimentation

$$Re = \frac{2\rho_f u_f H}{\mu_f}$$

$$Ar = \frac{\rho_f^2 (\rho_p / \rho_f - 1) g D_p^3}{\mu_f^2}$$

The boundary conditions in the x & z directions are periodic and in y-direction, no-slip condition with zero velocity is applied on the upper and lower wall. The pressure gradient is applied in the x-direction to drive the flow.

## Effect of initial particle configuration

In this section, the results for the effect of the particle configuration is presented. The simulations are carried out for 2 different cases - **Case 1:** The particles are stacked in three layers with each subsequent layer touching the layer below, **Case 2:** The particles are placed with a gap of  $D_p/2$  between each layer. Other relevant simulation parameters are summarized in Table 3.

**Table 3:** Simulation parameters used to study the effect of initial particle configuration

Simulation parameter	Value
# CV	300 x 160 x 60
# particles	135
$\Delta x$	0.01 m
$D_p/\Delta x$	20
Re	100
Ar	39.24
$\epsilon_s$	19.6 %

The simulation for both these cases is performed to study the behaviour of particles according to their initial configuration. It is found that for the given cases, the dynamics is substantially different although the non-dimensional parameters are kept constant (Figs. 4 & 5). It can be commented that for Case 2, the spacing between particles allows the particles to move freely due to gravity and lift forces affecting the flow field around it. With the evolution of time, the disturbance in the flow field leads to more pronounced asymmetric forces on the particles and consequently they remain in fluidized state (Fig. 5). On the contrary, no such fluidization is observed for Case 1 and particles remain sedimented during the entire simulation. This might be caused due to the restricted motion of particles in a closed packing. Hence, it is important to have a thin gap of fluid between particles to produce realistic simulations mimicking the proppant transport.

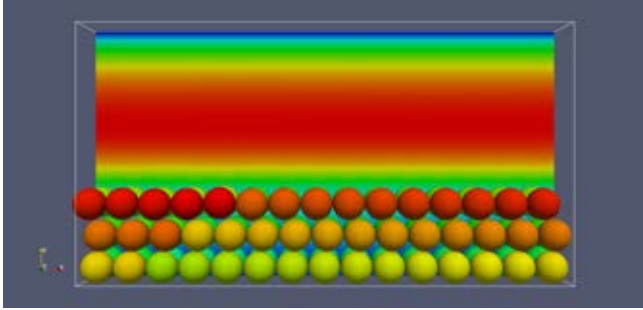


**Figure 4:** Particle configuration and the velocity distribution (on centre  $x$ - $y$  plane) at  $t^*(tu_f/D_p) = 17$  (Case 1)

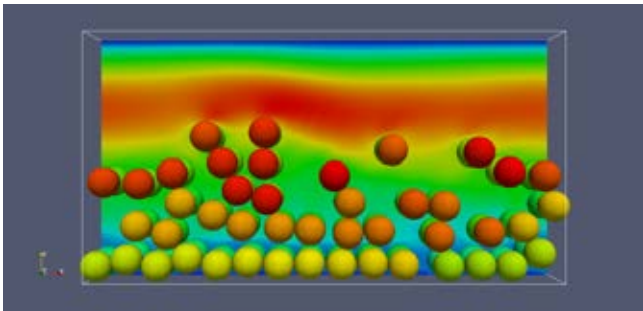
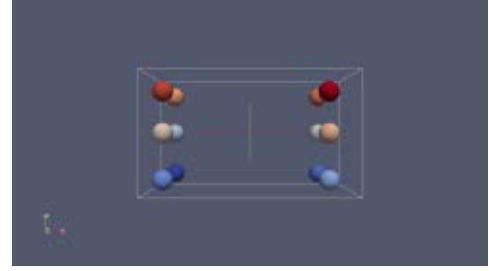


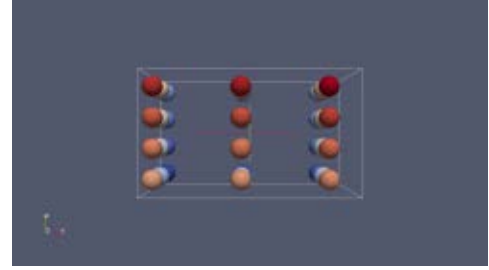
**Figure 5:** Particle configuration and the velocity distribution (on centre  $x$ - $y$  plane) at  $t^*(tu_f/D_p) = 17$  (Case 2)

### Effect of solids volume fraction

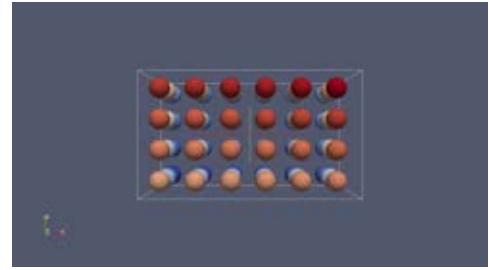
In this section, the effect of solids volume fraction on the particle transport and specifically, on the sedimentation times is studied. The initial particle configuration is shown in Fig. 6 whereas Table 4 lists the detailed simulation parameters.



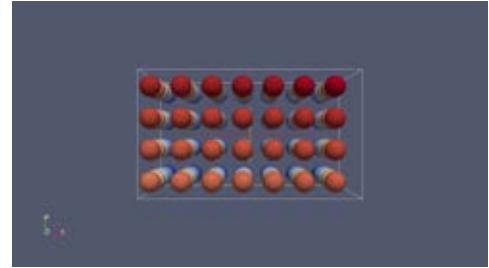
a)  $\epsilon_s = 0.017$



c)  $\epsilon_s = 0.05$



e)  $\epsilon_s = 0.1$



g)  $\epsilon_s = 0.2$

**Figure 6:** Initial configuration of particles for different solids volume fraction.

In these simulations, the average vertical location (Eq. 13) of all particles is monitored to obtain the sedimentation time. The time at which  $y_{avg}$  reaches a steady state value, is used as the sedimentation time and is listed in Table 5 for the chosen parameter space.

$$y_{avg} = \frac{1}{N} \sum_{n=i}^{n=N} y_i \quad (13)$$

The aim of the fracking process is to attain operating conditions with a longer sedimentation time such that particles are carried deeper into a fracture. It can be observed from the results that the sedimentation time increases by decreasing  $Ar$  owing to the reduced effect of the gravitation force. However,

**Table 4:** Simulation parameters used to study the effect of solids volume fraction

Simulation parameter	Value
# CV	200 x 120 x 120
$\Delta x$	0.01 m
$D_p/\Delta x$	20
Re	100 - 400
Ar	0-7848
$\epsilon_s$	1.7 - 20%

with the higher sedimentation times, it is also important for the particles not to fluidize in the flowback stage of the fracking process. The lighter particles will tend to fluidize quickly in the flowback and the efficiency of the process would be reduced. Hence, it would be important to use the heavier particles and still have a longer sedimentation time. From Table 5, it can be observed that the sedimentation time for  $Re = 400$  is comparable for the cases  $\{\epsilon_s = 0.017, Ar = 1569.6\}$  and  $\{\epsilon_s = 0.2, Ar = 7848\}$  which signifies that the heavier particles can also be transported at a longer distances if the higher solids volume fraction is used. The pattern for the influence of the Reynolds number on the sedimentation time is not consistent for all the volume fractions, however, the Reynolds number tends to increase the sedimentation time at higher value of  $\epsilon_s$ .

Ar \ Re	100	200	300	400
0	-	-	-	-
1569.6	13.4	11.2	10.5	9.3
3924	6.7	6.9	6.4	6.1
7848	3.9	4.2	4.7	4.8

a) Sedimentation time (s)  $\epsilon_s=0.017$ 

Ar \ Re	100	200	300	400
0	-	-	-	-
1569.6	20.2	24.7	23.4	35.2
3924	9.8	10.3	10	12.8
7848	4.7	5.3	6.1	7.4

b) Sedimentation time (s)  $\epsilon_s=0.05$ 

Ar \ Re	100	200	300	400
0	-	-	-	-
1569.6	21.1	25.6	23.2	18.3
3924	18.4	18.6	18.9	13.2
7848	8.7	9.1	10.2	7.6

c) Sedimentation time (s)  $\epsilon_s=0.1$ 

Ar \ Re	100	200	300	400
0	-	-	-	-
1569.6	17.2	15.2	22.4	23.2
3924	10.3	13.7	12.8	15.6
7848	8.6	12.6	9.9	11.3

d) Sedimentation time (s)  $\epsilon_s=0.2$ **Table 5:** Sedimentation time for all cases simulated, various  $\epsilon_s$ 

## CONCLUSION

In this work, an efficient and accurate model for the direct numerical simulation (DNS) of liquid-solid flows is presented. The torque computation results with the improved immersed boundary method (IBM) are presented for the single rotating sphere in a quiescent fluid in comparison with the original IBM. It is found that the improved IBM reduces the error around 3-13 times. The verified and validated IBM is then used to simulate the transport of solid particles in a narrow channel to mimic the proppant transport in rock fractures in a fracking process. Initially, the simulation of transport of 135 particles with two different particle arrangements is performed and it was found that the spacing between the particles leads to a fluidization, contrary to the packed particle system with the same non-dimensional flow parameters. Hence, it is important to have a gap between particles while performing simulations to attain closer similarity with the real process.

As a next step, 48 simulation cases are performed to study the influence of the solids volume fraction, Archimedes number and Reynolds number on the proppant transport phenomenon. It was found that the sedimentation time of the heavier particles can be increased by increasing the solids volume fraction and it is even comparable to the sedimentation time of the lighter particles in the dilute system. Moreover, the influence of increasing Reynolds number is more pronounced and consistent in the higher volume fraction cases and contributes positively to keep the particles fluidized for a longer period.

In reality, the process of proppant transport is quite complex due the rough walls in the rock fractures with the varying widths, visco-elastic fracking fluids, randomly oriented cracks, high aspect ratio in dimensions of a crack and polydispersity in the proppant sizes. Moreover, large number of particles are used in this process. Hence, the numerical model has to be extended with the complex boundary conditions for rough walls, visco-elastic flow modeling and polydispersity of particles. To simulate the larger system, full parallelization of the fluid solver as well as particle part is also very important.

## ACKNOWLEDGEMENTS

This work is supported by the programme 'Computational Sciences for Energy Research (CSER)' of the Foundation for Fundamental Research on Matter (FOM) which is now part of the Netherlands Organisation for Scientific Research Institutes (NWO-I). This research is also co-financed by Shell Global Solutions International B.V. We thank NWO and Dutch Supercomputing Consortium SURFsara ([www.surfsara.nl](http://www.surfsara.nl)) for granting us the computational time on Cartesius cluster.

## REFERENCES

- BIRD, R.B., STEWART, W.E. and LIGHTFOOT, E.N. (2007). *Transport phenomena*. John Wiley & Sons.
- BRENNER, H. (1961). “The slow motion of a sphere through a viscous fluid towards a plane surface”. *Chemical Engineering Science*, **16(3-4)**, 242–251.
- BREUGEM, W.P. (2012). “A second-order accurate immersed boundary method for fully resolved simulations of particle-laden flows”. *Journal of Computational Physics*, **231(13)**, 4469–4498.
- CHOI, H.G. and JOSEPH, D.D. (2001). “Fluidization by lift of 300 circular particles in plane poiseuille flow by direct numerical simulation”. *Journal of Fluid Mechanics*, **438**, 101–128.
- CUNDALL, P.A. and STRACK, O.D. (1979). “A discrete numerical model for granular assemblies”. *Geotechnique*, **29(1)**, 47–65.
- DAS, S., DEEN, N.G. and KUIPERS, J. (2016). “Immersed boundary method (ibm) based direct numerical simulation of open-cell solid foams: Hydrodynamics”. *AIChE Journal*.
- DEEN, N.G., KRIEBITZSCH, S.H.L., VAN DER HOEF, M.A. and KUIPERS, J.A.M. (2012). “Direct numerical simulation of flow and heat transfer in dense fluid-particle systems”. *Chemical Engineering Science*, **81**, 329–344.
- FADLUN, E., VERZICCO, R., ORLANDI, P. and MOHD-YUSOF, J. (2000). “Combined immersed-boundary finite-difference methods for three-dimensional complex flow simulations”. *Journal of Computational Physics*, **161(1)**, 35–60.
- KEMPE, T. and FRÖHLICH, J. (2012). “An improved immersed boundary method with direct forcing for the simulation of particle laden flows”. *Journal of Computational Physics*, **231(9)**, 3663–3684.
- PATANKAR, N., KO, T., CHOI, H. and JOSEPH, D. (2001). “A correlation for the lift-off of many particles in plane poiseuille flows of newtonian fluids”. *Journal of Fluid Mechanics*, **445**, 55–76.
- PESKIN, C.S. (1972). “Flow patterns around heart valves: a numerical method”. *Journal of Computational Physics*, **10(2)**, 252–271.
- TEN CATE, A., NIEUWSTAD, C., DERKSEN, J. and VAN DEN AKKER, H. (2002). “Particle imaging velocimetry experiments and lattice-boltzmann simulations on a single sphere settling under gravity”. *Physics of Fluids*, **14(11)**, 4012–4025.
- TSENG, Y.H. and FERZIGER, J.H. (2003). “A ghost-cell immersed boundary method for flow in complex geometry”. *Journal of Computational Physics*, **192(2)**, 593–623.
- UHLMANN, M. (2005). “An immersed boundary method with direct forcing for the simulation of particulate flows”. *Journal of Computational Physics*, **209(2)**, 448–476.